Journal of Photochemistry & Photobiology, B: Biology 220 (2021) 112215

Contents lists available at ScienceDirect

Journal of Photochemistry & Photobiology, B: Biology

journal homepage: www.elsevier.com/locate/jphotobiol

Photobiomodulation therapy combined with radiotherapy in the treatment of triple-negative breast cancer-bearing mice

Camila Ramos Silva [a], Camila de Almeida Salvego [a], Maria Elisa Rostelato [b], Carlos Alberto Zeituni [b], Martha Simões Ribeiro [a,*]

[a] Center for Lasers and Applications, Nuclear and Energy Research Institute (IPEN/ CNEN), Av. Prof. Lineu Prestes, 2242, 05508-000, Brazil
[b] Radiation Technology Center, Nuclear and Energy Research Institute (IPEN/CNEN), Av. Prof. Lineu Prestes, 2242, 05508-000, Brazil

ARTICLE INFO

Keywords:
4 T1 cells
Low-level laser therapy
Preclinical study
Red laser
Total blood count

ABSTRACT

This work investigated the effect of photobiomodulation therapy (PBM) combined with radiotherapy (RT) on triple-negative breast cancer (TNBC)-bearing mice. Female BALB/c mice received 4 T1 cells into a mammary fat pad. Local RT was performed with a total dose of 60 Gy divided into 4 consecutive sessions of 15 Gy. For PBM, a red laser was used in three different protocols: i-) single exposure delivering 150 $J.cm^{-2}$ (24 h after the last RT session), and ii-) radiant exposure of 150 $J.cm^{-2}$ or iii-) fractionated radiant exposure of 37.5 $J.cm^{-2}$ (after each RT session). Tumor volume, complete blood cell count, clinical condition, metastasis, and survival of animals were monitored during 3 weeks post-RT. Our results demonstrated that regardless of the protocol, PBM arrested the tumor growth, improved the clinical condition, and prevented hemolytic anemia. Besides, although PBM groups have exhibited a high neutrophil:lymphocyte ratio (NLR), they decreased the number of lung metastases and enhanced mouse survival. Worthy of note, PBM should be used along with the RT sessions in higher radiant exposures, since PBM at 150 $J.cm^{-2}$ per session significantly extended the survival rate. Together, these data suggest PBM could be a potential ally to RT to fight TNBC.

1. Introduction

Breast cancer is a worldwide health problem. According to the World Health Organization, approximately 2 million cases emerged in 2018, and it is considered the 5th main reason for cancer-associated death [1]. The development of this disease has been associated with age, genetic, endocrine, behavioral, and environmental causes [2]. Additionally, this type of cancer is highly metastatic, with a focus on the brain, bones, and, especially, the lungs. Nonetheless, there is a high cure rate when it is diagnosed at an early stage [2].

Triple-negative breast cancer (TNBC) is an aggressive breast cancer subtype defined by the absence of estrogen and progesterone receptors, and by the overexpression of the human epidermal growth factor receptor 2 gene (HER2). It mainly affects young women being responsible for 10 to 20% of all invasive breast cancers. Moreover, it is very resistant to current treatments [3]. Indeed, patients with recurrent TNBC have a poor prognosis and short life-expectancy compared to other breast cancer subtypes. In these cases, limitations in the treatment provide only a palliative care for the patients [4].

Currently, the available treatments for TNBC are chemotherapy, radiation therapy (RT), and mastectomy. The latter can be partial, radical, or total. The choice of treatment is based primarily on the stage of cancer and the condition of the patient, even though it frequently requires multimodal treatment [5–7].

RT consists of using X- or gamma rays to fight cancer growth, once these types of ionizing radiation (IR) have high tissue penetration and the ability to induce DNA damage to cancerous cells [8]. This modality is largely applied for TNBC treatment [5]. However, due to its radioresistance, high IR doses and a long treatment period are necessary, which may cause severe adverse effects and aggravate the patient's clinical and social conditions [6]. The most common adverse effects caused by RT are fatigue, skin burns, loss of appetite, nausea, vomiting, and low blood counts. Besides, a part of the rib and sternum can be in the area of irradiation contributing to the myelosuppression, a significant dose-limiting side effect of RT for patient-bearing breast cancer [9,10]. This might result in poor adherence to the RT, resulting in treatment failure and contributing to breast cancer progression. Thus, there is an urgent need to research new strategies to fight TNBC.

* Corresponding author.
E-mail address: marthasr@usp.br (M.S. Ribeiro).

https://doi.org/10.1016/j.jphotobiol.2021.112215
Received 25 January 2021; Received in revised form 31 March 2021; Accepted 14 May 2021
Available online 17 May 2021

In this context, photobiomodulation therapy (PBM), or as previously named low-level laser therapy, has been studied and reported in health sciences due to an international trend to look for less invasive therapeutic methods. In virtue of its beneficial effects, *e.g.,* acceleration of tissue repair [11], pain relief [12], promotion of welfare [13], more recently it has been applied as supportive care in breast cancer to treat the adverse effects of RT, such as radiodermatitis [14,15] and lymphedema [16]. The literature also supports the radiation-modifying effect of PBM in cell cultures and/or *in vivo* studies [17–20].

Herein, we developed a murine model of orthotopic breast cancer using 4 T1 cancer cells, which exhibit TNBC characteristics [21]. We evaluated the impact of PBM combined with RT on the tumor progression, clinical condition, metastasis, and survival rate. We also conducted an in-depth hematological study to investigate how PBM could assist RT.

2. Experimental

2.1. Cell Cultures

Cells of 4 T1 murine breast cancer (ATCC ® CRL-2539) were cultured in RPMI 1640 medium (Sigma, USA) supplemented with 10% fetal bovine serum (Sigma, USA), 100 U/mL penicillin, and 100 μg/mL streptomycin (Sigma, USA) at 37 °C in a humidified atmosphere with 5% CO_2. When a confluence of 70% was reached, the cells were detached using 0.25% trypsin and 0.03% ethylenediaminetetraacetic acid (EDTA) (Sigma, USA), quantified by the trypan blue exclusion method in a Neubauer chamber, and suspended at a concentration of 1×10^5 cells into 40 μL of the medium.

2.2. Animals and the Tumor

All experiments were performed following the Committee on Ethics in the Use of Animals (CEUA) guidelines (approval protocol n° 190/17) at the Energy and Nuclear Research Institute (IPEN). Female BALB/c mice with an initial body mass of approximately 20 g and 6–8 weeks age were housed under alternate dark and light cycles (12 h/12 h), with access to food and water *ad libitum*. The animals were anesthetized with 2.5% isoflurane by inhalation (Cristália, Brazil), trichotomized in the mammary gland region, and, after local asepsis, were inoculated with 1×10^5 4 T1 cells into the lower-left mammary fat pad, using a 1 mL syringe and 27- gauge hypodermic needle. This methodology allows the development of an orthotopic breast tumor [21]. The volume was monitored daily until it was palpable (about 0.1 cm^3 after 14 days of inoculation) by means of a digital caliper with an accuracy of mm. Eq. (1) was used to estimate the tumor volume [22]:

$$V(cm^3) = 0.5\ x\ length\ x\ width^2 \quad (1)$$

2.3. Radiotherapy (RT)

Local RT was performed using a panoramic Co-60 source from Radiation Technology Center at IPEN. As defined in a previous study [23], the total dose delivered to the target was 60 Gy divided into 4 consecutive fractions of 15 Gy per session. Before each session, animals were anesthetized intraperitoneally with xylazine (10 $mg.kg^{-1}$) and ketamine (100 $mg.kg^{-1}$) and accommodated into a lead shielding device specially developed for the assays [24].

2.4. Photobiomodulation Therapy

PBM was carried out on the tumor with a red laser (MMOptics Ltda, Brazil) ($\lambda = 660$ nm, power of 20 mW, spot area of 0.04 cm^2 and irradiance of 500 $mW.cm^{-2}$), in three protocols: i) single PBM exposure at 150 $J.cm^{-2}$ 24 h after the last session of RT (RT + PBM_{24}), and PBM applied immediately after each session of RT with ii) radiant exposure of 150 $J.cm^{-2}$ (RT + PBM) or iii) fractionated radiant exposure of 37.5 J. cm^{-2} (RT + PBM_F). To standardize the light delivered to the target, the red laser was positioned at 90° to the tumor center. The light dose was based on previous work, which showed that PBM at 150 $J.cm^{-2}$ after RT induces senescence of breast tumor cells [20].

Thirty mice were used in this study and randomly assigned to 5 groups as displayed in Table 1 ($N = 5$ animals/group).

2.5. Clinical Monitoring

The clinical condition of all animals was monitored weekly until week 3 post-RT when mice were euthanized. We assigned clinical scores to estimate the health condition of the animals based on five signs, as suggested by Fentener van Vlissingen and colleagues [25]. According to this methodology, the overall highest score indicates a critical or severe state of the animal, whereas the lowest score indicates a good health condition. The clinical aspects were evaluated by a veterinarian and scored as displayed in Table 2.

2.6. Complete Blood Count (CBC)

CBC was evaluated in weeks 0, 1, 2, and 3 post-RT, as shown in Fig. 1. Blood samples with approximately 30 μL were collected from the caudal vein and added into 1 μL of 10% sodium EDTA as an anticoagulant. Counts of red blood cells (RBCs), leukocytes, and platelets were determined using a veterinary hematologic cell counter 2800 BCE VET (Mindray, China). Differential leukocyte counts were carried out in pantochromatic stained blood smears and evaluated under optical microscopy [26].

2.7. Euthanasia and Organ Examination

Mice were euthanized in week 4 using an overdose of anesthetics (60 $mg.kg^{-1}$ xylazine and 235 $mg.kg^{-1}$ ketamine) according to the humane endpoint established. Lungs were collected postmortem and superficial lung metastatic sites were counted by visual inspection. Fig. 1 exhibits the timeline of the experimental procedure.

2.8. Statistical Analysis

Data distribution was verified by the Shapiro-Wilk test. For group comparisons, we performed the two-way analysis of variance (ANOVA) with repeated measures and Tukey as post-test using the Origin Pro 8.5 program. For the survival analysis, we used the Log-Hank test, and for the number of superficial lung metastases, one-way ANOVA was used. Results are presented as means ± standard error of the mean (SEM), and statistically significant differences were assumed when $p < 0.05$.

3. Results

3.1. PBM Arrests Tumor Growth and Sustains Better Clinical Scores than the RT Group

Fig. 2**a** shows the growth of the tumor volume during the experimental period. We noticed an exponential growth for all groups, and statistically significant differences were identified within-group over time and between groups for each experimental moment.

The tumor group exhibited a significant increase throughout the experimental period, while groups exposed to RT showed a significant increase only from week 2. Interestingly, all groups submitted to PBM maintained similar tumor volume in weeks 2 and 3.

Differences between groups were noticed since week 1 when the untreated tumor group showed a significant increase of 50% when compared to other groups. On the other hand, the RT/PBM and RT/PBM_F protocols arrested significantly the tumor development, which was 2-fold smaller than the RT group in week 2 (0.38 ± 0.05 cm^3 and 0.38 ± 0.07 cm^3 *versus* 0.76 ± 0.16 cm^3, respectively). This behavior

Table 1
Groups and parameters used in this study.

Group	Protocol of RT	Protocol of PBM	Radiant exposure/session (J.cm^{-2})	Exposure time/session (s)	Energy/session (J)
Healthy	No exposure	No exposure	0	0	0
Tumor	No exposure	No exposure	0	0	0
RT	4 × 15 Gy	No exposure	0	0	0
RT + PBM_{24}	4 × 15 Gy	PBM 24 h after the last session of RT (single exposure)	150	300	6
RT/ PBM	4 × 15 Gy	PBM immediately after each RT session (4 exposures)	150	300	6
RT/PBM_F	4 × 15 Gy		37.5	75	1.5

Table 2
Evaluated clinical aspects and their scores.

Clinical Aspect	Levels	Score
Loss of body mass	None	0
	5%	1
	10%	5
	20%	10
Hypokinesia	Normal activity	0
	Reduced activity	5
	Inactive	10
Hunching	Normal posture	0
	Hunched posture	1
Piloerection	None	0
	Piloerection	1
Respiration alteration	None	0
	With alteration	1

was maintained until week 3. Fig. 2 **b** illustrates the tumor size before euthanasia of animals.

Fig. 3 shows the mean clinical scores for each group during the experimental period. Clinical signs reflect directly the health condition of the animals. Untreated tumor-bearing mice showed hypokinesia, hunched posture, piloerection, breathing alteration, and worsened each week. The RT group showed a more pronounced score in week 0 but maintained the same clinical signs over time. In contrast, the groups treated with RT immediately followed by PBM showed a significant worsening only in week 3. On the other hand, comparisons within-time revealed that in week 1 all groups that received PBM exhibited a significantly lower clinical score than the tumor and RT groups. This behavior was maintained in week 2 for the RT/PBM and RT/PBM_F groups. In week 3, mice that received PBM along with RT (RT/PBM and RT/PBM_F) continued to show better clinical conditions compared to tumor and RT groups (4.80 ± 0.37 and 4.20 ± 1.52 *versus* 12.0 ± 1.0 and

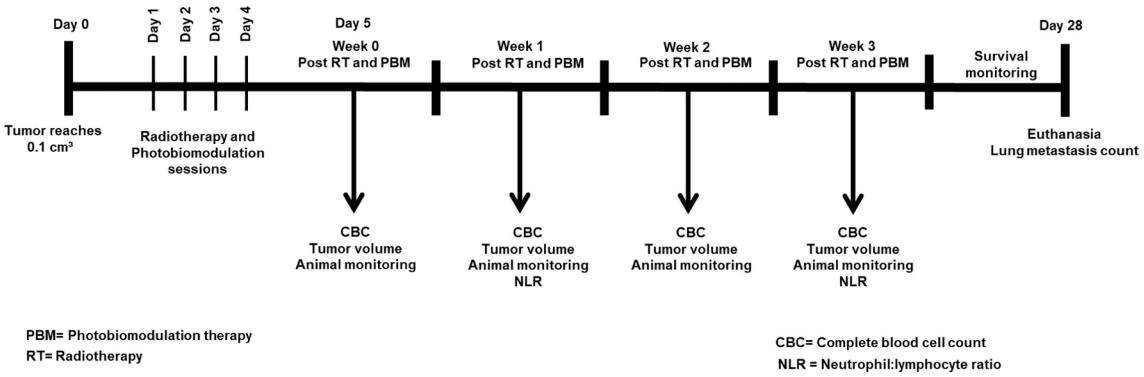

Fig. 1. Experimental design of this study.

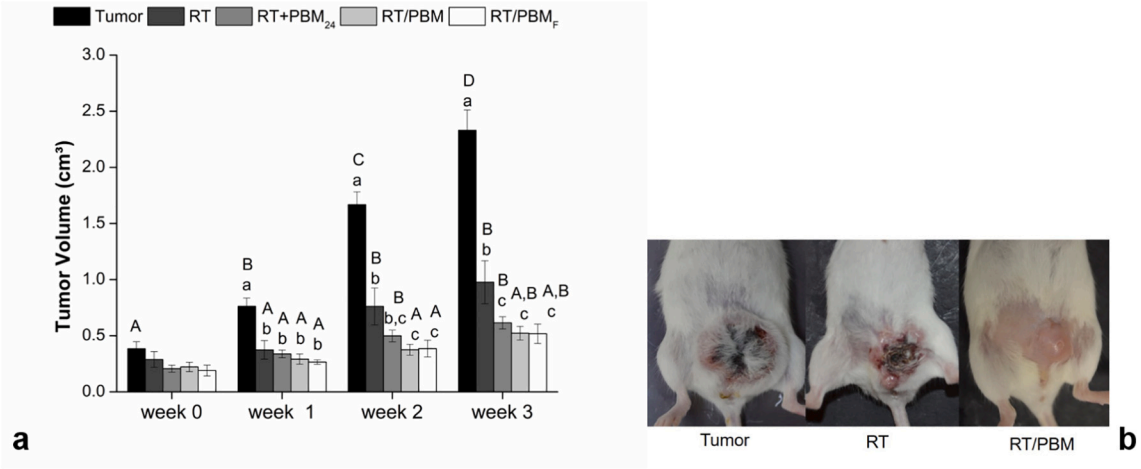

Fig. 2. (a) Tumor volume during the experimental period. Different uppercase letters (A, B, C, D) represent statistically significant differences within-group over time. Different lowercase letters (a, b, c) denote statistically significant differences between groups in each experimental period. Data are presented as mean ± SEM with 5 animals per group. (b) Representative images of mice-bearing 4 T1 breast cancer for tumor, RT, and RT/PBM groups before euthanasia. Observe that RT/PBM was able to arrest the tumor growth.

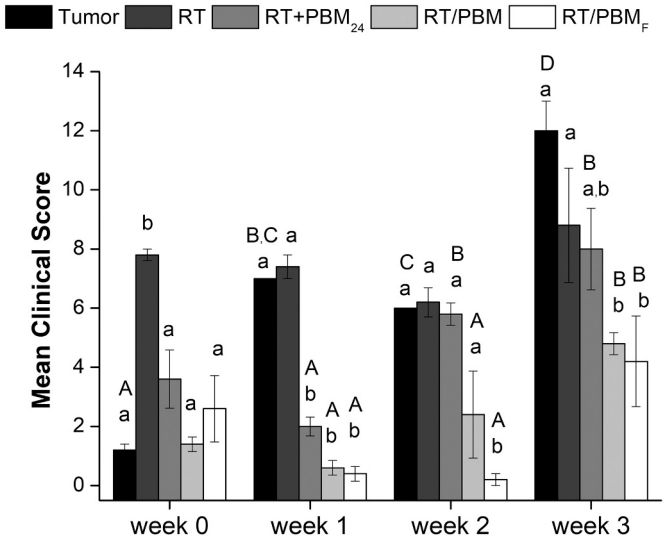

Fig. 3. Clinical score during the experimental period. Different uppercase letters (A, B, C, D) represent statistically significant differences within-group over time. Different lowercase letters (a, b) denote statistically significant differences between groups in each experimental period. Data are presented as mean ± SEM with $n = 5$ animals/group.

8.80 ± 1.93, respectively).

3.2. PBM Influences RBC Indices and Leukocytes

RBC counts exhibited similar behavior during the experimental period for the tumor and healthy mice groups (Fig. 4 **a**). On the other hand, mice exposed only to RT showed a decrease in RBC counts at week 2 and week 3 in comparison to week 0. Moreover, the RT groups combined with PBM presented a similar behavior over time, except the RT/PBM protocol, which showed a reduction in RBC counts only at week 1 compared to week 0.

Comparing the groups, we identified a statistically significant decrease in the RBC counts for all groups exposed to RT at week 1 when compared to healthy mice. However, on the 3rd-week post-RT, lower RBC levels were noticed for the RT ($7.87 \pm 0.82 \times 10^{12}$ L^{-1}) and RT/PBM$_F$ ($8.01 \pm 1.26 \times 10^{12}$ L^{-1}) groups when compared to the healthy mice ($11.88 \pm 0.32 \times 10^{12}$ L^{-1}).

Hemoglobin levels (Fig. 4 **b**) showed a significant decrease of approximately 27% in the RT group in week 3 when compared to week 0. This difference was also observed for the RT/PBM group between weeks 0 and 1 when the hemoglobin levels decreased around 28%. Additionally, all groups submitted to RT exhibited hemoglobin levels significantly lower than the tumor and healthy groups in week 1. However, in week 3, groups RT + PBM$_{24}$ and RT/PBM showed the same levels of hemoglobin as in week 1. Only the RT (12.30 ± 1.30 g.dL^{-1}) and RT/PBM$_F$ (12.40 ± 1.70 g.dL^{-1}) groups showed lower values compared to the healthy group (17.50 ± 0.40 g.dL^{-1}).

Hematocrit percentage is displayed in Fig. 4 **c**. In week 1 and week 3, the RT group showed a statistically significantly lower percentage of hematocrits than week 0. Besides, all groups exposed to RT showed lower hematocrit levels compared to the tumor and healthy groups in week 1. In week 3, statistically significant differences regarding the hematocrit percentage were observed for the RT (39.00 ± 4.50%) and RT/PBM$_F$ (43.00 ± 6.84%) groups compared to healthy mice (63.20 ± 2.08%).

RBC indices exhibited some differences during the experimental period (Table 3). The mean corpuscular volume (MCV) increased significantly between weeks 0 and 2 for the RT + PBM$_{24}$ and RT groups

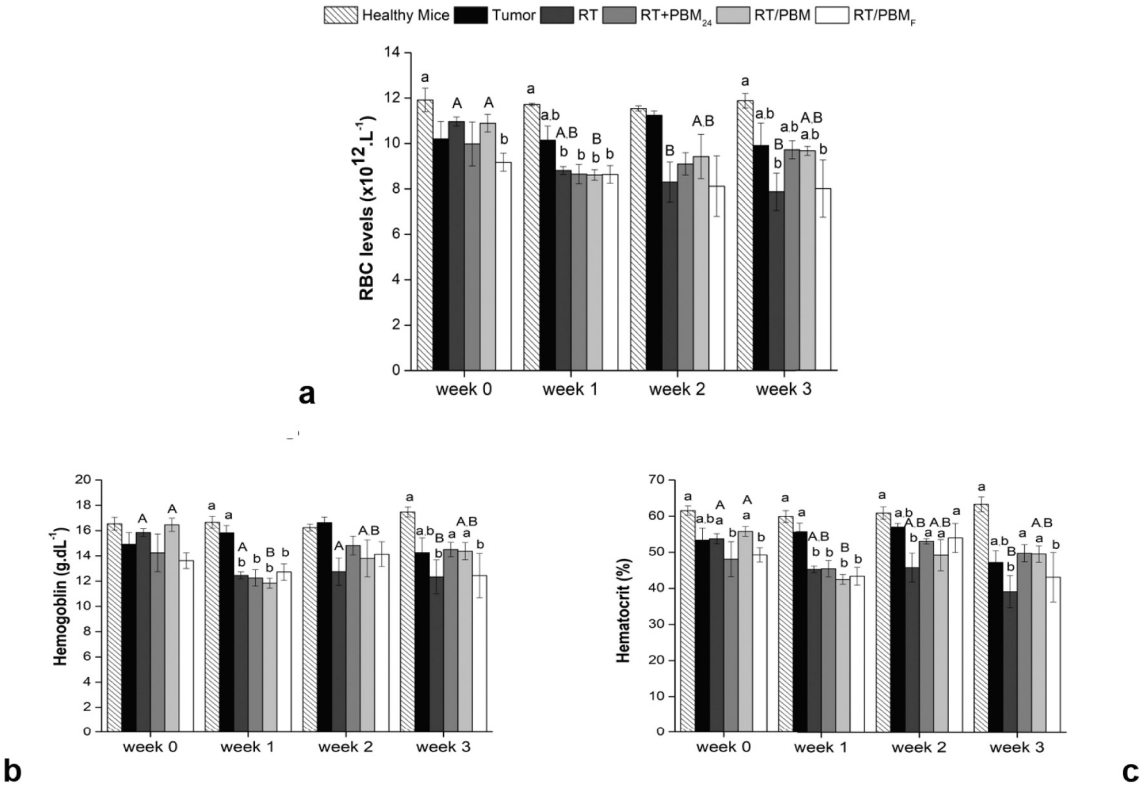

Fig. 4. Parameters of red blood cells analyzed during the experimental procedure. (a) RBC, (b) hemoglobin, and (c) hematocrit levels during the experimental period. Different uppercase letters (A, B, C) represent statistically significant differences within-group over time. Different lowercase letters (a, b) denote statistically significant differences between groups in each experimental period. Data are presented as mean ± SEM with $n = 5$ animals/group. (For interpretation of the references to colour in this figure legend, the reader is referred to the web version of this article.)

Table 3
RBC indices during the experimental period. Different uppercase letters (A, B, C) represent statistically significant differences within-group over time. Different lowercase letters (a, b) denote statistically significant differences between groups in each experimental period. Data are presented as mean ± SEM ($n = 5$ animals/group).

		MCV (fL)	MCH (pg)	MCHC (g/dL)	RDW (%)
Week 0	Healthy	54.78 ± 1.25^{a}	14.64 ± 0.08	26.82 ± 0.58^{a}	16.34 ± 0.60^{a}
	Tumor	53.50 ± 0.93^{a,b}	14.88 ± 0.12	27.9 ± 0.37 ^{a,b}	16.38 ± 0.47^{a}
	RT	49.04 ± 0.74^{Ab}	14.40 ± 0.14^{A}	29.44 ± 0.28 $^{A\ b}$	13.66 ± 0.39^{Ab}
	RT + PBM_{24}	48.18 ± 1.16^{Ab}	14.14 ± 0.28^{A}	29.52 ± 0.51^{b}	12.94 ± 0.39^{Ab}
	RT/PBM	49.68 ± 1.16^{a,b}	14.60 ± 0.26	29.46 ± 0.32^{b}	14.32 ± 0.12^{Aa,b}
	RT/PBM_F	54.2 ± 1.88^{a,b}	14.88 ± 0.04	27.64 ± 0.94^{a,b}	16.70 ± 1.01^{Aa}
Week 1	Healthy	52.66 ± 1.18	14.52 ± 0.07^{a}	27.78 ± 0.54	16.30 ± 0.38
	Tumor	51.52 ± 0.91	14.58 ± 0.15^{a}	28.04 ± 0.46	16.34 ± 0.45
	RT	51.34 ± 0.55	14.08 ± 0.13 ^{Aa}	27.54 ± 0.25 ^{Aa}	14.76 ± 0.43 $^{A,\ B}$
	RT + PBM_{24}	52.34 ± 1.11	14.08 ± 0.18 ^{Aa}	27.00 ± 0.36	14.6 ± 0.13 ^{A}
	RT/PBM	49.26 ± 1.11	13.66 ± 0.15^{a,b}	27.90 ± 0.42	14.46 ± 0.60 ^{A}
	RT/PBM_F	50.20 ± 1.08^{A}	14.66 ± 0.18^{a}	29.42 ± 0.44^{b}	14.64 ± 0.65 ^{A}
Week 2	Healthy	55.24 ± 2.42	14.66 ± 0.24^{a}	26.74 ± 0.77	17.04 ± 1.04
	Tumor	50.9 ± 1.82	14.80 ± 0.10^{a}	29.27 ± 1.09	15.93 ± 0.12
	RT	55.75 ± 3.20^{B}	15.45 ± 0.44^{A,Ba}	27.92 ± 0.98$^{A,\ B}$	16.88 ± 0.99^{B}
	RT + PBM_{24}	57.20 ± 3.10^{B}	16.16 ± 0.19^{Ba,b}	28.60 ± 1.35	16.68 ± 0.81^{A,B}
	RT/PBM	52.56 ± 3.10	14.58 ± 0.21^{a}	27.92 ± 0.74	16.32 ± 0.51^{B}
	RT/PBM_F	59.82 ± 2.47^{B}	15.62 ± 0.43^{a}	26.24 ± 0.45	18.94 ± 1.12^{A,B}
Week 3	Healthy	53.20 ± 1.91	14.64 ± 0.37	27.68 ± 0.54^{a}	15.52 ± 0.37^{a}
	Tumor	50.05 ± 1.37	15. 02 ± 0.10	30.18 ± 0.71^{b}	17.5 ± 0.51^{a}
	RT	49.52 ± 1.37	15.60 ± 0.41^{B}	31.64 ± 0.76^{Bb}	19.3 ± 0.95 ^{Ca,b}
	RT + PBM_{24}	51.12 ± 1.27	14.90 ± 0.40^{A}	29.30 ± 1.02 ^{a}	18.62 ± 0.60 ^{Ba,b}
	RT/PBM	51.12 ± 1.27	14.8 ± 0.63	29.04 ± 0.53 ^{a}	19.00 ± 0.34^{Ca,b}
	RT/PBM_F	54.06 ± 1.82	15.80 ± 0.53	29.38 ± 1.21 ^{a}	20.32 ± 0.32^{b}

MCV: Mean corpuscular volume; **MCH**: Mean corpuscular volume; **MCHC**: Mean corpuscular hemoglobin concentration; **RDW**: Red cell distribution width.

and between weeks 1 and 2 for the RT/PBM_F group. Intergroup differences within-time were noticed only in week 0 for both RT + PBM_{24} and RT groups compared to the healthy group.

Regarding the mean corpuscular hemoglobin (MCH), values increased over time for both RT + PBM_{24} and RT groups. In week 1, a significant reduction was observed for the RT/PBM in comparison to the other groups. In week 2, the RT + PBM_{24} group exhibited an opposite behavior when compared to RT/PBM and healthy groups, *i.e.,* higher MCH counts. The mean corpuscular hemoglobin concentration (MCHC) showed statistically significant differences over time only for the RT group, while intergroup differences were noticed in weeks 0, 1, and 3.

Concerning the red cell distribution width (RDW), we observed statistically significant differences over time for the RT + PBM_{24}, RT/PBM, RT/PBM_F, and RT groups, which showed a significant increase in the percentage of RDW in weeks 2 and 3 compared to weeks 0 and 1. Additionally, all groups submitted to RT showed a higher percentage of RDW than the healthy mice on the 3rd week.

Regarding blood platelets, although we have identified a significant decrease in their counts for all groups exposed to RT in week 1, the platelet counts in week 3 were similar to those of week 0 (Fig. 5). In the 1st week, the tumor group showed statistically significantly lower platelet levels than the healthy group ($685.2 \pm 43.0 \times 10^{9}.L^{-1}$ *versus* $1497.4 \pm 199.9 \times 10^{9}.L^{-1}$), as well as all groups submitted to RT showed lower platelet counts than the tumor group. In weeks 0, 2 and 3, no statistically significant differences were noticed between groups.

All groups submitted to RT showed a significant increase in total leukocyte counts from week 2, except the RT/PBM group, which presented a significant increase only in week 3 (Fig. 6). Yet, all groups exposed to the RT showed lower leukocyte counts than tumor and healthy groups in week 0. In weeks 1 and 2, all groups submitted to RT showed lower counts than the tumor group, even though the tumor group presented higher levels than healthy mice. Besides, all groups showed similar leukocyte levels in week 3, and statistically significantly higher counts than healthy mice.

Leukocyte differential counts were performed and analyzed in weeks 1 and 3 post-RT (Fig. 7). We noted that lymphocyte levels decreased over time for all experimental groups, including healthy mice, as well as all groups submitted to RT showed lower lymphocyte counts (about 60%) than healthy and tumor groups in week 1 (Fig. 7 **a**). Additionally, the tumor and RT-exposed groups presented approximately 4-fold lower lymphocyte counts than healthy group in week 3.

Monocyte counts (Fig. 7 **b**) decreased over time, except for the healthy mice. We also noticed that monocyte counts were significantly higher for groups that received RT in week 1. In the 3rd week, all groups showed similar monocyte counts, and no statistically significant differences were detected.

Different from lymphocytes, neutrophil counts increased in week 3. Nevertheless, healthy mice and the RT/PBM group maintained their values over time (Fig. 7 **c**). All groups showed neutrophil counts significantly higher than healthy mice, except the RT/PBM group, in week 3.

Regarding the neutrophil-lymphocyte ratio (NLR), all groups presented similar values in week 1. However, we observed a significant increase for the groups that received PBM in week 3 (Fig. 7 **d**). Additionally, the RT/PBM group showed a significant increase in the NLR (22.33 ± 4.87) when compared to the healthy (0.41 ± 0.05), tumor (6.77 ± 1.28), and RT (8.48 ± 1.56) groups in week 3 post-RT.

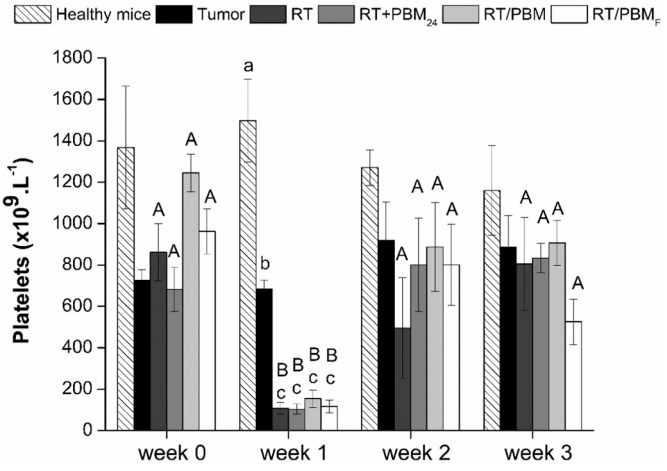

Fig. 5. Blood platelet levels during the experimental period. Different uppercase letters (A, B) represent statistically significant differences within-group over time. Different lowercase letters (a, b) denote statistically significant differences between groups in each experimental period. Data are presented as mean ± SEM with $n = 5$ animals/group.

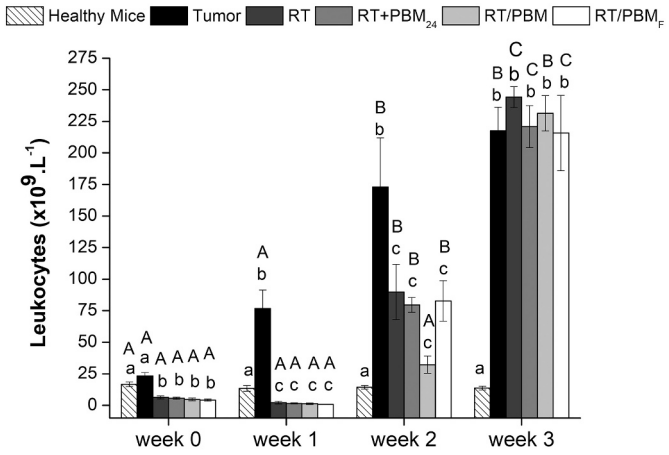

Fig. 6. Leukocyte levels during the experimental period. Different uppercase letters (A, B, C) represent statistically significant differences within-group over time. Different lowercase letters (a, b, c) denote statistically significant differences between groups in each experimental period. Data are presented as mean ± SEM with $n = 5$ animals/group.

Fig. 8 displays representative images obtained from blood smear of breast tumor-bearing mice and represent the differential leukocyte counts on the 3rd experimental week. Regardless of the analyzed group, platelets and some platelet aggregates were observed. Moreover, for the experimental groups, the number of neutrophils was more pronounced than the healthy group. We also noticed a moderate quantity of smudge cells for the tumor (Fig. 8 **b**) and RT (Fig. 8 **c**) groups.

3.3. PBM Promotes a Lower Number of Lung Metastases and Extends the Survival of Mice

Fig. 9**a** shows the curves for animal survival of the experimental groups. We can observe that mice from the tumor and RT groups started to die on day 24, and both groups achieved 60% of survival on day 28. On the other hand, the RT + PBM_{24} and RT/PBM_F groups showed 20% deaths. Interestingly, a statistically significant difference was noticed between the RT/PBM group and the tumor and RT groups. The RT/PBM group presented 100% of survival at the end of the experimental period.

Regarding lung metastases, we noticed that all groups exposed to PBM exhibited a significantly lower number of metastatic nodules than the tumor and RT groups (6.5 ± 3.7, 3.0 ± 1.2, and 8.0 ± 2.2 *versus* 20.7 ± 2.3 and 24.3 ± 6.2, respectively) (Fig. 9 **b and c**).

4. Discussion

In this work, we have successfully induced TNBC in female BALB/c mice. Then, animals were treated with a high dose of RT fractionated in 4 sessions. After that, the PBM was applied in 3 protocols to verify if and how it could assist RT. We noticed that the RT arrested tumor progression and caused injuries to the bone marrow since low blood cell counts were detected for RT-exposed groups in week 1. Moreover, we noted that PBM promoted smaller tumor volume than RT, improved clinical conditions, extended survival rate, reduced metastatic nodules in the lungs, and increased NLR, especially the RT/PBM group.

Our data confirm that tumor progression is directly related to the health condition of the animals as the larger the tumor, the worse the mouse clinical signs [27]. However, although the RT group has presented a smaller tumor size than the tumor group, it significantly promoted higher clinical scores than the PBM/RT and PBM/RT_F groups at the end of the study. This finding could be explained by the adverse side effects caused by whole breast RT as fatigue [28]. These results indicate that when PBM is applied along with the RT sessions, regardless of the light dose, it could improve the quality of life of patients with TNBC.

CBC is considered an oncological protocol for monitoring the patient's health condition and breast tumor progression [29]. As previously reported, we noticed that RT damaged the bone marrow preventing the production of blood cells. Indeed, it was expected since

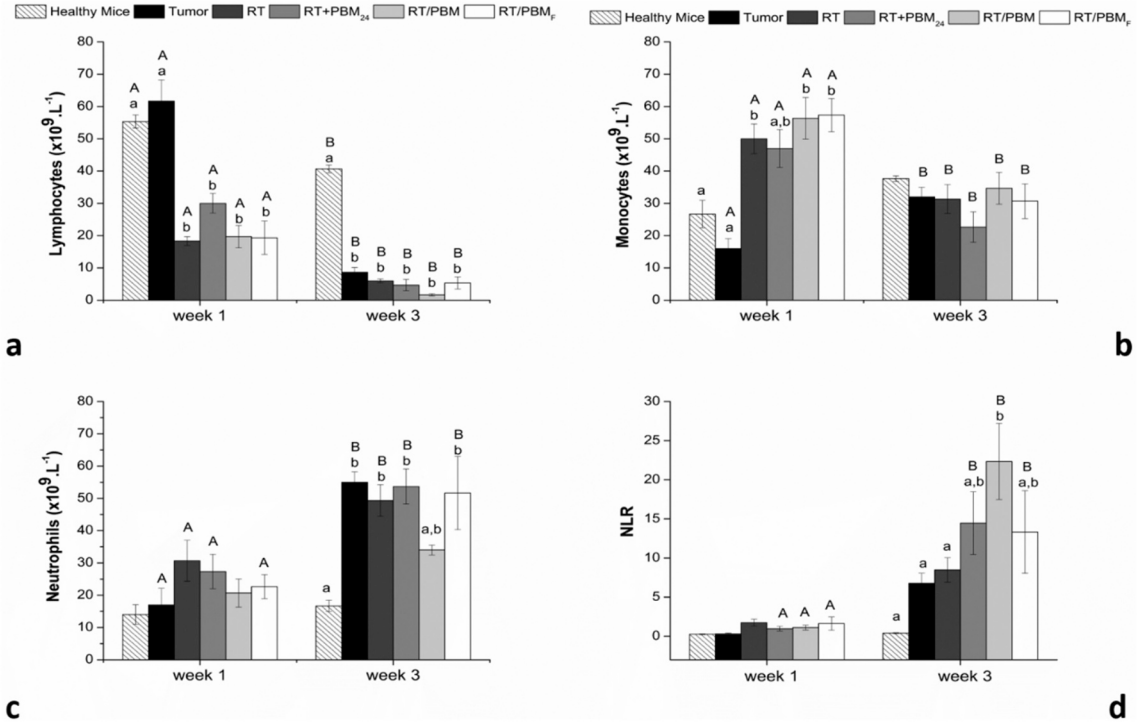

Fig. 7. Mean values ± SEM of the absolute count of (a) lymphocytes, (b) monocytes, (c) neutrophils, and (d) neutrophil:lymphocyte ratio during weeks 1 and 3. Different uppercase letters (A, B) represent statistically significant differences within-group over time. Different lowercase letters (a, b) denote statistically significant differences between groups in each experimental period. Data are presented as mean ± SEM with $n = 5$ animals per group.

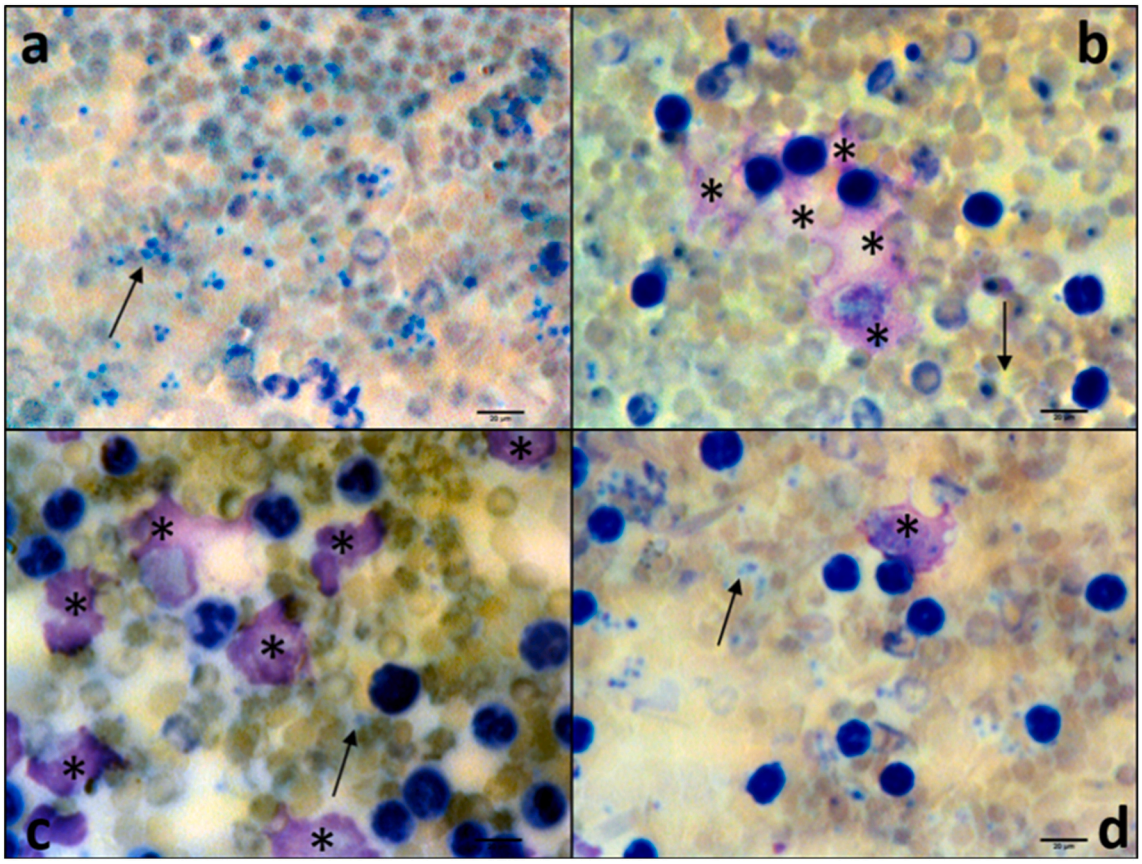

Fig. 8. Photomicrographs of the differential leukocyte count for (a) healthy mice (b) tumor (c) RT and (d) RT/PBM groups in week 3. Smudge cells are represented by asterisks, and platelets are indicated by arrows. Rosenfeld staining. Bar = 20 μm.

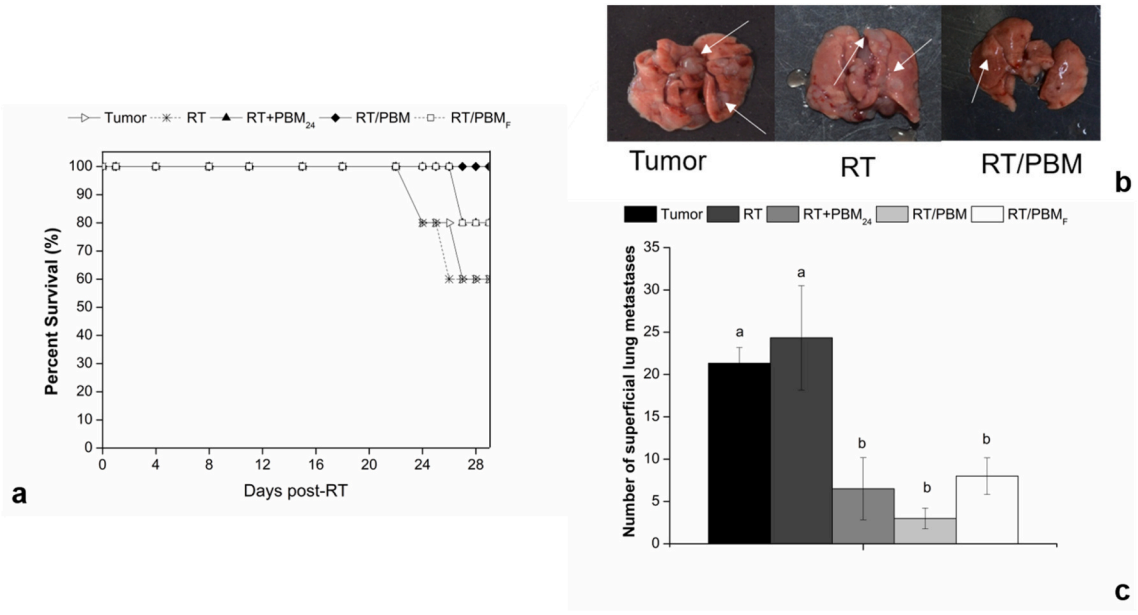

Fig. 9. a) Survival curves for experimental groups during 28 days post-RT. Statistically significant differences were observed between RT/PBM and RT and tumor groups with $p = 0.04$; b) Representative images of mouse lungs after euthanasia for the tumor, RT, and RT/PBM groups. The arrows point to the metastatic nodules; c) Mean values ± SEM of the number of superficial lung metastatic nodules for the experimental groups. Different lowercase letters (a, b) represent statistically significant differences between groups.

IR is scattered to other organs, even with the shielding to target the breast tumor [24]. Thus, mice exposed to RT acquired short-lived aplastic anemia since CBCs increased over time [30].

However, all experimental groups displayed levels of erythrocytes, hemoglobin, and hematocrits below the reference interval in week 3. This finding is in agreement with the tumor development, which

impedes medullar erythropoiesis by granulocyte colony-stimulating factor and then causes anemia in 4 T1 breast tumor-bearing mice [31]. Yet, Sohier and collaborators were pioneers in reporting the appearance of anemia with hemolytic characteristics in the late stage of the disease for 4 patients with breast cancer [32]. Interestingly, the MCHC index, which measures the average concentration of hemoglobin inside a single red blood cell, was significantly higher than reference values (24.5–29.4 g/dL) only for the tumor and RT groups. As an elevated MCHC may be indicative of the presence of hemolysis [33], we hypothesize that PBM might prevent hemolytic anemia by arresting the tumor growth and mitigating RT adverse effects. Further evidence is warranted to clarify this issue.

Leukocytes are considered to be defense cells and changes in their counts in circulation could indicate the progression of breast cancer [34]. Thus, the monitoring and differentiation of leukocytes are routine in an oncological protocol. In our study, leukocyte levels exhibited a significant increase during the experimental period, although a slower evolution was observed for the groups exposed to RT until week 2. This finding is also consistent with the murine model of 4 T1-induced breast cancer, which prompts a leukemoid reaction with granulocytosis [35]. We also noticed smudge cells in smear blood, more pronounced in tumor and RT groups. Smudge cells normally are fragile lymphocytes, which may be damaged in the physical process of making a smear or be related to chronic lymphocytic leukemia (CLL) [36]. However, the RT of solid tumors still has not been associated with CLL [37].

The lymphocyte and monocyte counts decreased between the first and third weeks, while the neutrophils increased regardless of the PBM protocol. A prior study demonstrated that lymphocytes exhibit a faster response to IR as a possible consequence of radiation-induced cell death [38]. Moreover, the increase of neutrophils is expected, since neutrophils can be associated with cancer progression and metastases [39].

The literature has described NLR as an important prognostic marker. Indeed, it can provide an immediate representation of the inflammatory process, playing an important role in tumor growth, progression, invasion, and metastasis [40]. According to our results, PBM promoted an increase of the NLR values indicating a poor prognosis for TNBC-bearing mice. Although these findings are conflicting, it is noteworthy that for metastatic breast cancer the NLR should be not considered as an independent predictor of survival, since it seems to depend on other prognostic clinical factors [41]. Furthermore, circulating neutrophils may exhibit an antitumor activity and mount an antimetastatic response [42].

Hamblin and colleagues reported that there are three possible ways in which PBM could act against cancer cells [43]. One of these mechanisms would be a possible role in the stimulation of the immune system. Besides that, Ottaviani and collaborators have reported that PBM applied directly to a melanoma tumor upregulated type I IFNs cytokines, which possess an anti-proliferative, pro-apoptotic, and anti-angiogenic profile and play a pivotal role in immunosurveillance of cancer [44]. Thus, we assume that PBM, in this work, influenced the immune system of animals, recruiting neutrophils with antitumor activity, since we noticed a decrease the tumor volume and the number of lung metastases. Our findings also suggest that PBM should be applied along with the RT sessions in higher radiant exposures considering that 150 $J.cm^{-2}$ promoted longer survival.

In conclusion, this work is a first attempt to verify the effect of PBM combined with RT in the treatment of TNBC-bearing mice, providing valuable data to assist clinical practice. Regardless of the protocol, PBM was able to prevent tumor progression, mitigate the adverse effects promoted by the RT, and decrease the number of metastatic nodules in the lungs. Furthermore, the highest radiant exposure applied along with the RT sessions significantly extended the mouse survival. Taken together, these key findings motivate further studies to unravel the mechanisms behind and properly establish the safe use of PBM combined with RT to advance successful TNBC treatment.

Declaration of Competing Interest

The authors declare that they have no known competing financial interests or personal relationships that could have appeared to influence the work reported in this paper.

Acknowledgments

We thank Prof. Marcelo L. Santoro, Butantan Institute, São Paulo, Brazil for providing the use of the hematologic cell counter. We also thank Valdirene M. Barbosa (Butantan Institute) and Saulo T. Pereira (IPEN) for their technical assistance. This work was funded by Comissão Nacional de Energia Nuclear (CNEN) and the Instituto de Fotônica do Conselho Nacional de Desenvolvimento Científico e Tecnológico (INFO/CNPQ grant# 465763/2014-6). C. R. Silva was supported by scholarship from CNEN.

References

[1] F. Bray, J. Ferlay, I. Soerjomatarm, Global cancer statistics 2018: GLOBOCAN estimates of incidence and mortality worldwide for 36 cancers in 185 countries, CA Cancer J. Clin. 68 (2019) 394–424.
[2] N. Harbeck, F. Penault-Llorca, J. Cortes, M. Gnant, N. Houssami, P. Poortmans, et al., Breast cancer, Nat. Rev. Dis. Primers. 5 (2019) 66.
[3] P. Kumar, R. Aggarwal, An overview of triple-negative breast cancer, Arch. Gynecol. Obstet. 293 (2016) 247–269.
[4] A.R.T. Bergin, S. Loi, Triple-negative breast cancer: recent treatment advances, F1000Res 8 (2019). F1000 Faculty Rev-1342.
[5] S. Al-Mahmood, J. Sapiezynski, O.B. Garbuzenko, T. Minko, Metastatic and triple-negative breast cancer: challenges and treatment options, Drug Deliv. Transl. Res. 8 (2018) 1483–1507.
[6] L. He, Y. Lv, Y. Song, B. Zhang, The prognosis comparison of different molecular subtypes of breast tumors after radiotherapy and the intrinsic reasons for their distinct radiosensitivity, Cancer Manag. Res. 11 (2019) 5765–5775.
[7] J. Ju, A. Zhu, P. Yuan, Progress in targeted therapy for breast cancer, Chronic. Dis. Transl. Med. 4 (2018) 164–175.
[8] E.V. Maani, C.V. Maani, Radiation therapy. *StatPearls[Internet]*, Available at: https://www.ncbi.nlm.nih.gov/books/NBK537036/, 2020.
[9] D.E. Green, C.T. Rubin, Consequences of irradiation on bone and marrow phenotypes, and its relation to disruption of hematopoietic precursors, Bone 0 (2014) 87–94.
[10] Q. Wang, T. Ye, H.-L. Chen, X.-G. Zhang, L.-Z. Zhang, Correlation between intensity modulated radiotherapy and bone marrow suppression in breast cancer, Eur. Rev. Med. Pharmacol. Sci. 20 (2016) 75–81.
[11] C. Martignago, C. Tim, L. Assis, A. Andrade, P. Brassolati, P. Bossini, et al., Preemptive treatment with photobiomodulation therapy in skin flap viability, J. Photochem. Photobiol. B Biol. 201 (2019) 111634.
[12] G. Pigatto, C. Silva, N. Parizotto, Photobiomodulation therapy reduces acute pain and inflammation in mice, J. Photochem. Photobiol. B Biol. 196 (2019) 111513.
[13] J.T. Hashmi, Y.Y. Huang, B.Z. Osmani, S.K. Sharma, M.A. Naeser, M.R. Hamblin, Role of low-level laser therapy in neurorehabilitation, PM R 2 (2010) S292–S305.
[14] S. Censabella, S. Claes, J. Robijns, P. Bulens, J. Mebis, Photobiomodulation for the management of radiation dermatitis: the DERMIS trial, a pilot study of MLS((R)) laser therapy in breast cancer patients, Support Care Cancer 24 (2016) 3925–3933.
[15] J. Robijns, S. Censabella, S. Claes, L. Pannekoeke, L. Bussé, D. Colson, et al., Biophysical skin measurements to evaluate the effectiveness of photobiomodulation therapy in the prevention of acute radiation dermatitis in breast cancer patients, Support Care Cancer 27 (2019) 1245–1254.
[16] G.D. Baxter, L. Liu, S. Petrich, A.S. Gisselman, C. Chapple, J.J. Anders, et al., Low level laser therapy (Photobiomodulation therapy) for breast cancer-related lymphedema: a systematic review, BMC Cancer 17 (2017) 833.
[17] E. Cherkasova, K. Babak, A. Belotelov, J. Labutina, V. Yusupov, N. Vorobieva, et al., Effects of photobiomodulation in relation to HeLa Kyoto tumor cells exposed to ionizing radiation, J. Photochem. Photobiol. B Biol. 209 (2020) 111936.
[18] N. Morcos, M. Omran, H. Ghanem, M. Elahdal, N. Kamel, E. Attia, Phototherapeutic effect of low-level laser on thyroid gland of gamma-irradiated rats, Photochem. Photobiol. 91 (2015) 942–951.
[19] G.E. Djavid, B. Bigdeli, B. Goliaei, A. Nikoofar, M.R. Hamblin, Photobiomodulation leads to enhanced radiosensitivity through induction of apoptosis and autophagy in human cervical cancer cells, J. Biophotonics 10 (2017) 1732–1742.
[20] C. Ramos Silva, F.V. Cabral, C.F. de Camargo, S.C. Nunez, T. Mateus Yoshimura, A. C. de Lima Luna, et al., Exploring the effects of low-level laser therapy on fibroblasts and tumor cells following gamma radiation exposure, J. Biophotonics 9 (2016) 1157–1166.
[21] P. Kaur, G.M. Nagaraja, H. Zheng, D. Gizachew, M. Galukande, S. Krishnan, et al., A mouse model for triple-negative breast cancer tumor-initiating cells (TNBC-TICs) exhibits similar aggressive phenotype to the human disease, BMC Cancer 12 (2012) 120.

[22] K. Matsumoto, N. Obara, M. Ema, M. Horie, A. Naka, S. Takahashi, et al., Antitumor effects of 2-oxoglutarate through inhibition of angiogenesis in a murine tumor model, Cancer Sci. 100 (2009) 1639–1647.
[23] C.R. Silva, Preclinical Evaluation of the Photobiomodulation Combined to Radiotherapy in the Treatment of Breast Cancer. Ph.D. Thesis, University of São Paulo, Brazil, 2020.
[24] C.R. Silva, S.T. Pereira, C.M. Napolitano, E.R. Somessari, M.S. Ribeiro, Development of a shielding device for radiotherapy of breast cancer-bearing mice, Brazil. J. Rad. Sci. 8 (2020) 1–9.
[25] J.M. Fentener van Vlissingen, M. Borrens, A. Girod, P. Lelovas, F. Morrison, Y. S. Torres, The reporting of clinical signs in laboratory animals: FELASA working group report, Lab. Anim. 49 (2015) 267–283.
[26] A.T.A. Sachetto, J.G. Rosa, M.L. Santoro, Rutin (quercetin-3-rutinoside) modulates the hemostatic disturbances and redox imbalance induced by Bothrops jararaca snake venom in mice, PLoS Negl. Trop. Dis. 12 (2018), e0006774.
[27] A.I. Faustino-Rocha, M. Ginja, R. Ferreira, P.A. Oliveira, Studying humane endpoints in a rat model of mammary carcinogenesis, Iran J. Basic. Med. Sci. 22 (2019) 643–649.
[28] M. Pérez, M. Schootman, L.E. Hall, D.B. Jeffe, Accelerated partial breast irradiation compared with whole breast radiation therapy: a breast cancer cohort study measuring change in radiation side-effects severity and quality of life, Breast Cancer Res. Treat. 162 (2017) 329–342.
[29] Y. Shinden, K. Sugimachi, F. Tanaka, K. Fujiyoshi, Y. Kijima, S. Natsugoe, et al., Clinicopathological characteristics of disseminated carcinomatosis of the bone marrow in breast cancer patients, Mol. Clin. Oncol. 8 (2018) 93–98.
[30] N.S. Young, Aplastic anemia, N. Engl. J. Med. 379 (2018) 1643–1656.
[31] M. Liu, X. Jin, X. He, L. Pan, X. Zhang, Y. Zhao, Macrophages support splenic erythropoiesis in 4T1 tumor-bearing mice, PLoS One 10 (2015), e0121921.
[32] W.D. Sohier Jr., E. Juranies, J.C. Aub, Hemolytic anemia, a host response to malignancy, Cancer Res. 17 (1957) 767–774.
[33] S. Buys, C. Craven, MCHC in intravascular hemolysis, Am. J. Hematol. 33 (1990) 282–283.
[34] L. Chen, X. Kong, C. Yan, Y. Fang, J. Wang, The research progress on the prognostic value of the common hematological parameters in peripheral venous blood in breast cancer, Onco. Targets Ther. 13 (2020) 1397–1412.
[35] S.A. DuPré, D. Redelman, K.W. Hunter Jr., The mouse mammary carcinoma 4T1: characterization of the cellular landscape of primary tumours and metastatic tumour foci, Int. J. Exp. Pathol. 88 (2007) 351–360.
[36] G.L. Gulati, V. Uppal, G. Gong, J., Feasibility of counting smudge cells as lymphocytes in differential leukocyte counts performed on blood smears of patients with established or suspected chronic lymphocytic leukemia/small lymphocytic lymphoma, Lab. Med. 48 (2017) 137–147.
[37] T. Radivoyevitch, R.K. Sachs, R.P. Gale, M.R. Smith, B.T. Hill, Ionizing radiation exposures in treatments of solid neoplasms are not associated with subsequent increased risks of chronic lymphocytic leukemia, Leuk. Res. 43 (2016) 9–12.
[38] D.R. Heylmann, F. Kindler, T. Kain, B., Radiation sensitivity of human and murine peripheral blood lymphocytes, stem and progenitor cells, BBA Cancer Rev. 1846 (2014) 121–129.
[39] R. Grecian, M.K.B. Whyte, S.R. Walmsley, The role of neutrophils in cancer, Br. Med. Bull. 128 (2018) 5–14.
[40] J.L. Ethier, D. Desautels, A. Templeton, P.S. Shah, E. Amir, Prognostic role of neutrophil-to-lymphocyte ratio in breast cancer: a systematic review and meta-analysis, Breast Cancer Res. 19 (2017) 2.
[41] A.I. Rubio, J.C. Yufera, P.D.L. Morena, A.F. Sánchez, E.N. Manzano, E.G. Garre, et al., Neutrophil-lymphocyte ratio in metastatic breast cancer is not an independent predictor of survival, but depends on other variables, Sci. Rep. 9 (2019) 1–9.
[42] M.A. López-Lago, S. Posner, V.J. Thodima, A.M. Molina, R.J. Motzer, et al., Neutrophil chemokines secreted by tumor cells mount a lung antimetastatic response during renal cell carcinoma progression, Oncogene. 32 (2013) 1752–1760.
[43] M.R. Hamblin, S.T. Nelson, J.R. Strahan, Photobiomodulation and cancer: what is the truth? Photomed. Laser Surg. 36 (2018) 241–245.
[44] G.M. Ottaviani, V. Rupel, K. Caronni, N. Naseem, A. Zandona, L. Perinetti, et al., Laser therapy inhibits tumor growth in mice by promoting immune surveillance and vessel normalization, EBioMedicine 11 (2016) 165–172.